Dynamics of temporal attention and expectation revealed by continuous tracking of visual cortical responses

Rachel N. Denison*[1,2], Karen Tian*[1,2], David J. Heeger[1], Marisa Carrasco[1]
[1]New York University, [2]Boston University
* co-first authors

Corresponding author:
Rachel N. Denison
rdenison@bu.edu

Department of Psychological and Brain Sciences
Boston University
64 Cummington Mall
Boston, MA 02215
United States

Keywords: temporal attention, temporal expectation, magnetoencephalography, steady state visual evoked response

Abstract

In processing a stream of visual information, visual perception is improved by temporal expectation, the timing predictability of sensory events, and by voluntary temporal attention, the prioritization of sensory events at behaviorally relevant time points. Although temporal expectation and attention are often treated as a single process, they can be dissociated and may be supported by distinct neural mechanisms. Here, we manipulated temporal attention while holding expectation constant and used concurrent MEG to disentangle their effects on visual cortical dynamics. Human observers attended to one of two sequentially presented visual targets embedded in flickering noise on each trial. Using the intertrial phase coherence (ITPC) of visually responsive channels as a measure of cortical response reliability, we found two neural signatures of temporal expectation and attention in visual cortical responses. First, a ramping increase in ITPC anticipated the temporally expected onset of visual targets whether attended or not, with the slope of the ramp modulated by temporal attention. Second, the transient evoked ITPC response to the first visual target was larger when that target was temporally attended. These data reveal distinct and complementary impacts of temporal attention and expectation on visual cortical responses across time.

Introduction

We can often anticipate the points in time at which sensory events will be relevant for our behavioral goals. For example, when returning a tennis serve, it is critical to see the ball at the moment it hits your opponent's racket; only seeing the ball half a second earlier or later would be unhelpful. This prioritization of sensory information at specific points in time is temporal attention. In the case of the tennis serve, we attend in a goal-directed manner to the relevant time point, an example of voluntary temporal attention.

Voluntary temporal attention affects behavior by both improving perceptual sensitivity and speeding reaction times to attended stimuli (Correa et al., 2005; Davranche et al., 2011; Denison et al., 2021, 2017; Fernández et al., 2019; Miniussi et al., 1999; Nobre and Ede, 2018; Rohenkohl et al., 2014; Samaha et al., 2015). However, the neural mechanisms underlying these perceptual improvements are unknown. One reason for this knowledge gap is that previous neural studies have simultaneously manipulated temporal attention –the relevance of an upcoming stimulus time– and temporal expectation –the predictability of an upcoming stimulus time– although it has been shown in visual spatial and feature-based attention, as well as in audition, that relevance and predictability can have distinct behavioral and neural effects (Bang and Rahnev, 2017; Cheadle et al., 2015; Hillyard et al., 1998; Kok et al., 2012; Lange and Röder, 2006; Richter et al., 2018; Rungratsameetaweemana and Serences, 2019; Summerfield and Egner, 2016, 2009; Todorovic et al., 2015; Wyart et al., 2012). In the domain of visual temporal attention, we have found that voluntary temporal attention improves performance (Denison et al., 2021, 2017; Fernández et al., 2019) and affects microsaccades (Denison et al., 2019) over and above the effects of expectation. These results also suggest dissociable neural mechanisms.

A commonly observed neural signature of expectation is a slow ramping activity, increasing over the course of hundreds of milliseconds to several seconds, that peaks around the time of an anticipated event. A variety of ramping signals have been observed in cortical and subcortical areas (Finnerty et al., 2015; Leon and Shadlen, 2003; Maimon and Assad, 2006; Merchant et al., 2013). However, expectation-related ramping activity has rarely been observed in visual areas (Lima et al., 2011), and whether ramps in neural activity depend on temporal attention has not been investigated.

In contrast to a gradual ramp, our normalization model of dynamic attention predicts that voluntary temporal attention changes the gain of visual responses rapidly and transiently, roughly coincident with the evoked sensory response to the visual stimulus (Denison et al., 2021). These model dynamics were constrained by psychophysical data showing that voluntary temporal attention to a visual stimulus affected perceptual sensitivity even when sequential stimuli were separated by intervals of only 250 ms (Denison et al., 2021, 2017; Fernández et al., 2019). A slow ramping modulation of visual responses may not allow such temporally precise attentional selection.

Here we investigated how temporal attention dynamically modulates visual cortex by continuously tracking visual cortical responses using MEG while human observers performed a voluntary temporal attention task. To measure attentional modulations continuously across time, it is necessary to continuously drive the visual cortex. We did so by presenting a 20 Hz flickering noise patch throughout each trial, which produces a steady-state visual evoked response (SSVER) at 20 Hz in the visual cortex. We measured time-resolved visual cortical responses throughout the trial by calculating the inter-trial phase coherence (ITPC) at the steady-state frequency, as ITPC is the primary driver of SSVER power (Ding et al., 2006; Kashiwase et al., 2012; Kim et al., 2007; Moratti et al., 2007). ITPC in response to a periodic stimulus depends on how consistently the stimulus drives a neural response across trials. ITPC can therefore be considered a measure of

neural response reliability. Both ITPC (Kashiwase et al., 2012; Kim et al., 2007) and SSVER amplitude (Morgan et al., 1996; Müller et al., 1998b, 1998a; Norcia et al., 2015) have been shown to be modulated by spatial attention. Here we used an SSVER approach to study temporal attention. Further, we used a task protocol that allowed us to measure the effects of voluntary temporal attention over and above those of temporal expectation. A precue directed attention to one of two sequential targets that were presented at fixed, predictable times.

We found signatures of both temporal expectation and attention in visual cortex activity. Consistent with previous psychophysical results (Denison et al., 2021, 2017; Fernández et al., 2019), perceptual sensitivity depended on the precue, with higher perceptual sensitivity for the first and marginally higher perceptual sensitivity for the second of two sequential targets when each was attended vs. unattended. In the neural data, temporal expectation changed visual cortical responses in anticipation of the predictable target stimuli in the form of a slow ramping modulation of visual cortical ITPC. Voluntary temporal attention had two, separate effects on visual cortical ITPC. First, temporal attention affected the slope of the ramp, with a steeper slope when the first of the two targets was attended. Second, temporal attention selectively increased the transient ITPC response to the first target when it was attended, in line with the prediction of the normalization model of dynamic attention (Denison et al., 2021). The effect of this attentional modulation was to change the relative response magnitudes of the first and second targets, according to the attentional precue. The results unify previous findings by showing how ramping mechanisms contribute to temporal expectation and how both ramping and transient modulatory mechanisms contribute to temporal attention. The presence of these dynamic modulations in visually-driven cortical activity suggests a mechanism for how temporal expectation and attention can affect visual perceptual sensitivity.

Results

Temporal precueing improved perceptual sensitivity

To investigate the effects of voluntary temporal attention and temporal expectation on visual cortical dynamics, we recorded MEG while observers performed a temporal attention task with fully predictable stimulus timing (**Figure 1**). Observers directed temporal attention to one of two sequential grating targets separated by a 300 ms stimulus onset asynchrony (SOA) and discriminated the orientation of one grating on each trial. A precue tone at the start of each trial instructed observers to attend to either the first target (T1) or second target (T2), and a response cue tone at the end of each trial instructed observers to report the tilt (clockwise or counterclockwise) of one of the targets. The response cue matched the precue with 75% validity, so observers had incentive to direct their attention to different points in time according to the precue.

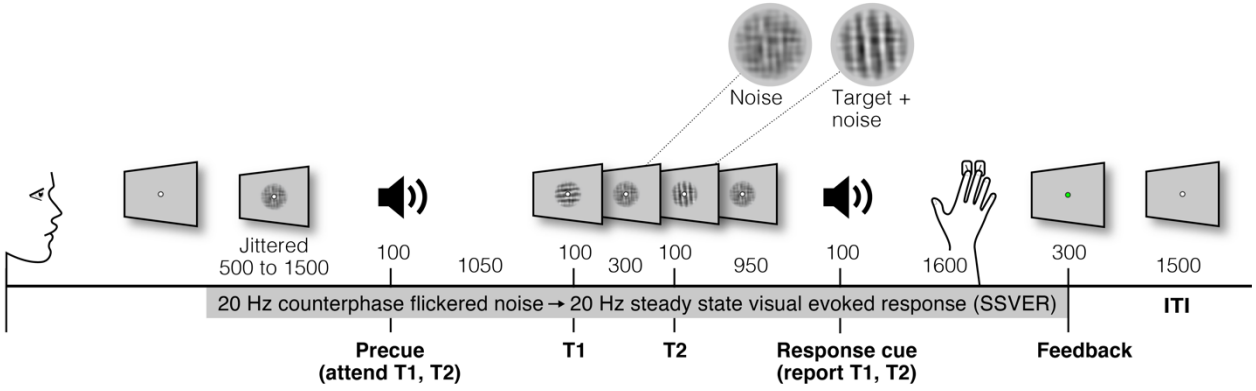

Figure 1. Temporal cueing task. Trial timeline showing stimulus durations and SOAs in ms. Targets were embedded in 20 Hz counterphase flickering noise. Precues and response cues were pure tones (high = cue T1, low = cue T2).

Temporal attention improved orientation discrimination performance, consistent with previous findings (Denison et al., 2021, 2017; Fernández et al., 2019; Rohenkohl et al., 2014; Samaha et al., 2015). Perceptual sensitivity (*d'*) was higher overall for valid trials (when the response cue matched the precue) than invalid trials (when the response cue did not match) (main effect of validity: F(1,9) = 8.03, p = 0.02, η_G^2 = 0.25) (**Figure 2**). Perceptual sensitivity for T1 was higher than that for T2 (main effect of target: F(1,9) = 16.47, p = 0.0028, η_G^2 = 0.261). No other main effects or interactions were found for *d'* (F(1,9) < 3.05, p > 0.11). Given the directional nature of time, we also tested how temporal attention affected each target separately. The improvement in *d'* with temporal attention was significant for T1 individually (F(1,9) = 9.08, p = 0.01, η_G^2 = 0.38; valid: mean *d'* = 1.79, SD = 0.44; invalid: mean *d'* = 1.21, SD = 0.88) with a trend for improvement for T2 (F(1,9) = 4.75, p = 0.06, η_G^2 = 0.20; valid: mean *d'* = 1.20, SD = 0.39; invalid: mean *d'* = 0.85, SD = 0.61). Reaction time (RT) was faster for valid versus invalid trials overall (F(1,9) = 39.87, p < 0.001, η_G^2 = 0.76) and for each target individually ([T1: F(1,9) = 43.02, p < 0.001, η_G^2 = 0.79; valid: mean RT = 0.62 s, SD = 0.23 s; invalid: mean RT = 0.89 s, SD = 0.23 s] ,[T2: F(1,9) = 34.71, p < 0.001, η_G^2 = 0.74; valid: mean RT = 0.63 s, SD = 0.24 s; invalid: mean RT = 0.88 s, SD = 0.22 s]). No other main effects or interactions were found for RT (F(1,9) < 2.66, p > 0.14) (**Figure 2**). Thus, we can rule out any speed-accuracy tradeoffs in the effect of the precue on performance.

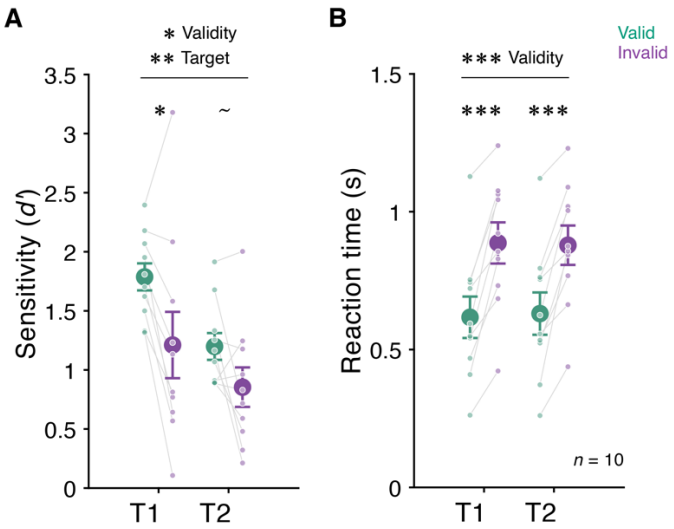

Figure 2. Behavior. Mean (**A**) perceptual sensitivity and (**B**) reaction time for each target (T1, T2) by attention condition. Sensitivity was higher and reaction time faster for valid (green) than invalid (purple) trials. Error bars indicate ± 1 SEM. ~ p < 0.1; * p < 0.05; ** p < 0.01; *** p < 0.001.

Continuous tracking of visual responses using ITPC

To allow continuous tracking of visual responses as observers deployed temporal attention and expectation, we used an SSVER protocol. The grating targets were embedded in a stream of 20 Hz counterphase flickering noise, filtered to have similar orientation and spatial frequency content as the targets. The targets were presented superimposed on the noise background for 100 ms each and also flickered at 20 Hz in phase with the ongoing noise flicker. This protocol allowed visual cortical responses to be tracked throughout the trial by measuring the 20 Hz SSVER.

For each observer, we first measured the 20 Hz SSVER power for each channel, calculated from the average time series across all trials (henceforth "trial-average power"), and selected the five most visually responsive channels for further analysis. As expected, the most visually responsive channels were located in the back of the head, consistent with occipital responses (**Figure 3A**). We confirmed strong 20 Hz trial-average power in these channels and found that power was enhanced specifically at the 20 Hz stimulus frequency (**Figure 3C**).

Trial-average power depends on two factors: 1) single-trial power and 2) phase coherence across trials at the frequency of interest, or ITPC (**Figure 3B**). Therefore, we next asked how the 20 Hz SSVER depended on these two factors. As in previous studies that have pulled apart ITPC and single-trial power (Ding et al., 2006; Kashiwase et al., 2012; Kim et al., 2007; Moratti et al., 2007), we found that ITPC was the dominant component of the trial-average SSVER, with a strong and specific 20 Hz ITPC response (**Figure 3E**). Single-trial power had a relatively weak 20 Hz component and was dominated by alpha power around 10 Hz (**Figure 3D**). We therefore used ITPC as our primary measure to quantify responsiveness to visual stimulation in our subsequent analyses.

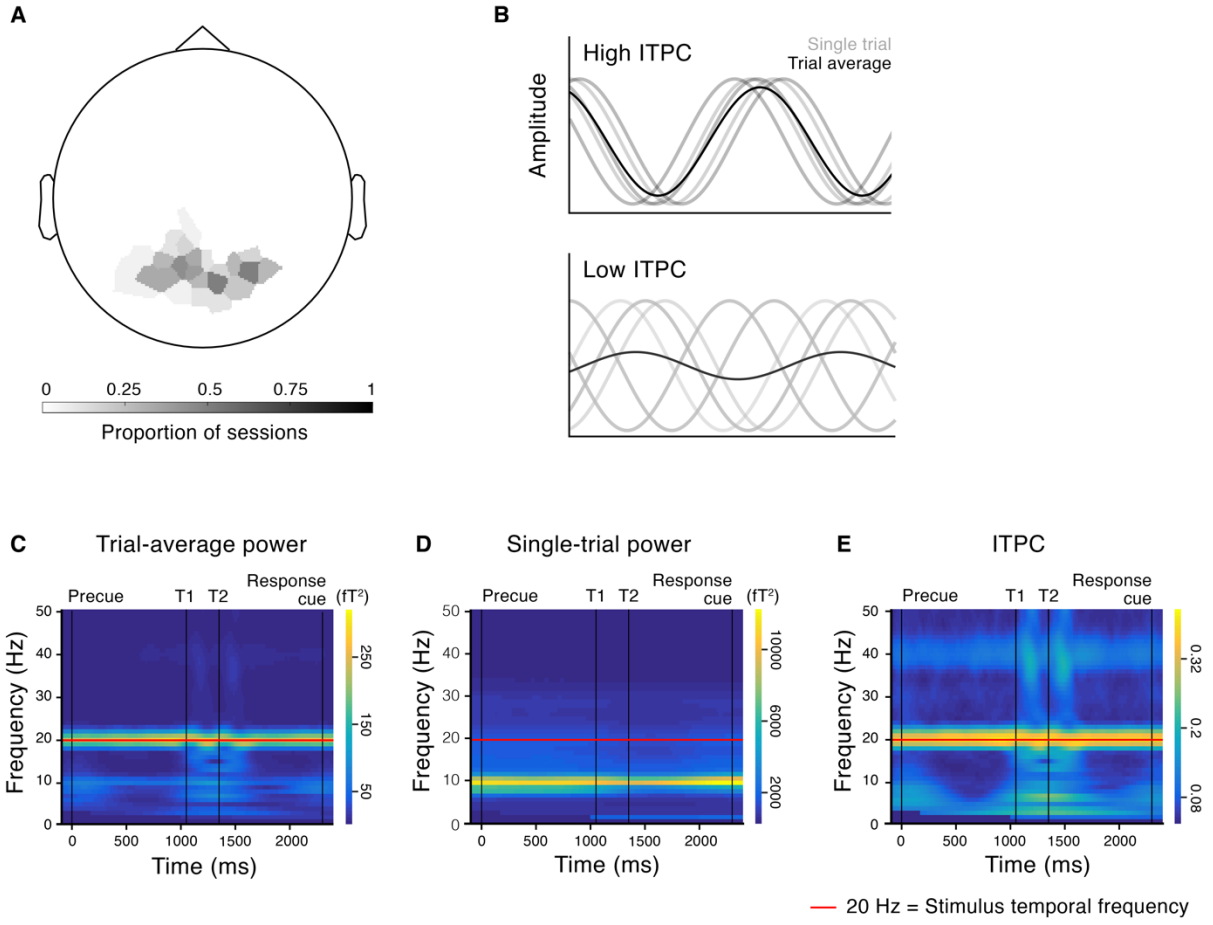

Figure 3. MEG responses to steady-state visual stimulation. (**A**) Topography of visually responsive channels across observers (top five channels selected for each session based on 20 Hz trial-average SSVER power). Grayscale indicates the proportion of sessions across observers in which the channel was selected as visually responsive. (**B**) Illustration of cartoon time series from five trials (gray) and their average (black). High phase coherence across trials results in high ITPC and trial-average power (top); low phase coherence across trials results in low ITPC and trial-average power (bottom), despite the same single-trial

power. (**C-E**) Time frequency spectrograms of (**C**) trial-average power reveals a strong 20 Hz signal at the stimulus frequency. Trial-average power depends on two factors: (**D**) the power on single trials and (**E**) phase coherence across trials, or ITPC. The trial-average power at 20 Hz was more strongly reflected in ITPC than in single-trial power.

Temporal expectation was accompanied by a ramping increase in ITPC

We first asked how temporal expectation (regardless of attention) affected ITPC in the period between the precue and the first target. In all trials, a predictable interval of 1.05 s elapsed between the onset of the precue and the onset of T1, so observers could form an expectation about the timing of T1 onset (Denison et al., 2019, 2017; Fernández et al., 2019). We observed an apparent neural signature of expectation in the form of a slow ramping increase of ITPC (mean slope = 0.045 ΔITPC/s, SD = 0.043) during the precue-to-T1 period (**Figure 4A, Supplementary Figure 1**). To quantify the rate of increase, we fit lines to each observer's ITPC time series from the onset of the precue to 80 ms before T1 (a cushion before T1 was inserted to prevent responses to T1 from interfering with the fit, see Methods). The slope of the ITPC time series was positive for 8/10 observers and significantly greater than zero across the group ($F(1,9) = 3.31$, $p = 0.009$, $\eta_G^2 = 0.40$) (**Figure 4B**). In contrast, single-trial power showed no ramping increase in the precue-to-T1 period (**Supplementary Figure 1C**), confirming that a ramping increase in cortical response reliability was the critical factor driving the change in ITPC.

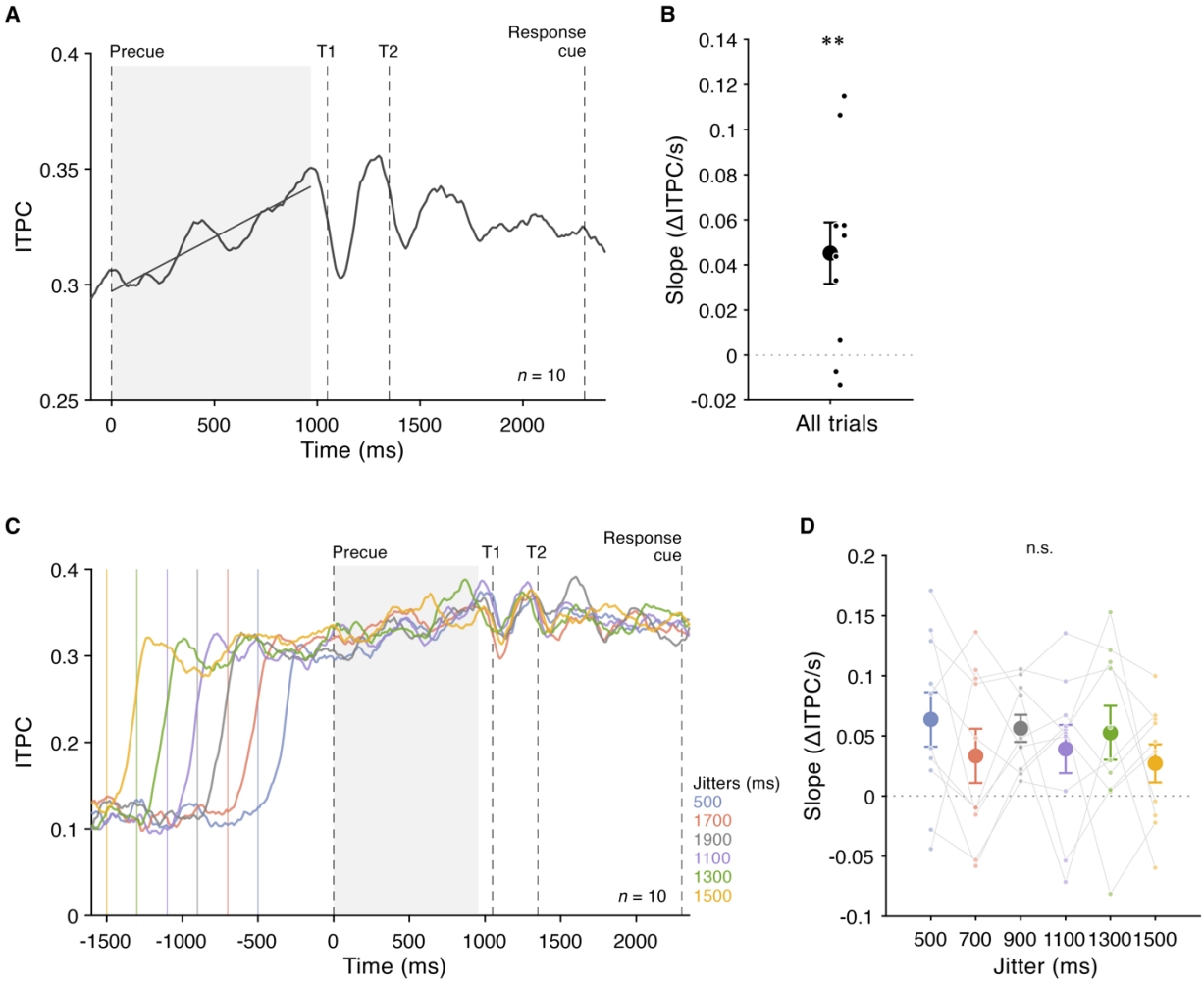

Figure 4. Ramping increase in ITPC associated with temporal expectation. (**A**) Mean 20 Hz ITPC time series across all trials (*n* = 10). Lines were fit to each observer's ITPC time series during the precue-to-T1 period (gray shading). Linear fit to group data (gray line) shown for visualization. (**B**) Fitted slopes for each observer and group mean. (**C**) ITPC ramp is time-locked to the precue. Mean 20 Hz ITPC time series (*n* = 10) for each jittered duration of SSVER stimulation before the precue. Colored vertical lines indicate the onset of the stimulus flicker for each duration. (**D**) ITPC slopes during the precue-to-T1 period were similar for all jitter durations. Large data points show the group means, and small data points show individual data, with each observer's data points connected by lines. Error bars are ±1 SEM. ** p < 0.01 compared to zero.

To ensure this ITPC ramp was locked to the precue and not simply the continuous build-up of the SSVER signal, we separated trials according to the duration of the SSVER stimulation period before the precue, which had been jittered from 500 to 1500 ms to prevent predictable precue timing. A one-way ANOVA revealed no significant differences in ITPC slope across the six jitter durations ($F(1,9) = 1.19$, $p = 0.30$, $\eta_G^2 = 0.03$). (**Figure 4C,D**). Therefore, the ITPC ramp was evidently initiated by the precue and indicates a gradual increase in visual cortical response reliability tied to expectation.

Temporal attention modulated the rate of anticipatory ramping of ITPC

We next asked whether temporal attention—over and above expectation—affects the anticipatory increase in ITPC as the target onset time approaches. Whereas expectation reflects the predictability of visual events, attention incorporates the task-relevance of events (Denison et al., 2021, 2019; Fernández et al., 2019; Summerfield and Egner, 2016, 2009). In the present experimental design, temporal expectation was constant across all trials, because the two targets always appeared at the same, predictable times. Temporal attention, however, varied with the precue.

We therefore asked whether the precue affected the ramping response reliability in advance of the targets. To do so, we fit lines to each observer's ITPC time series during the precue-to-T1 period, with separate fits for precue T1 and precue T2 trials. (Note that we could only characterize ramping signals before T1, because the interval between T1 and T2 is short and contains the evoked response to T1.) We found that the slope was steeper for precue T1 trials (mean slope = 0.058 ΔITPC/s, SD = 0.057) than for precue T2 trials (mean slope = 0.032 ΔITPC/s, SD = 0.049). The magnitude of the difference in slope was 56% of the overall rate of increase and reliable across observers ($F(1,9) = 7.60$, $p = 0.022$, $\eta_G^2 = 0.16$). This result indicates that temporal attention acts over and above expectation to modulate anticipatory ramping of ITPC depending on the timing of upcoming task-relevant targets (**Figure 5**).

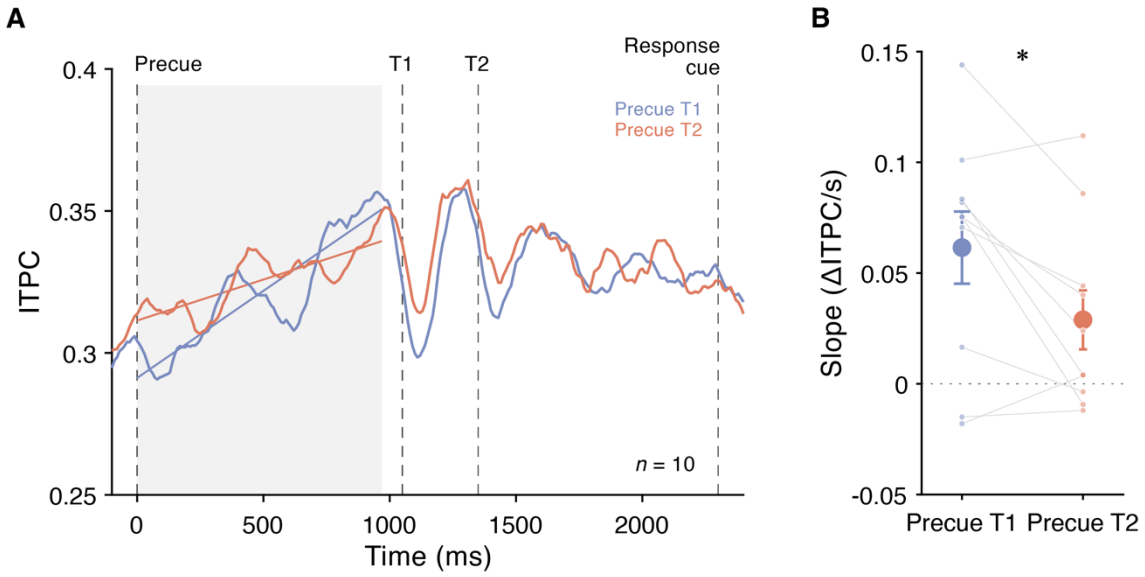

Figure 5. Anticipatory effect of precue on ITPC. (**A**) Mean 20 Hz ITPC time series for each precue type (*n* = 10). Lines were fit to each observer's ITPC time series during the precue-to-T1 period (gray shading). Linear fits to group data (red and blue lines) shown for visualization. (**B**) Temporal attention affected the ramping ITPC leading up to the first target. Fitted slopes were larger for precue T1 trials than for precue T2 trials. Error bars indicate ± 1 SEM. * $p < 0.05$.

The target-evoked ITPC response varied across observers but was stable within observers

Having characterized the ITPC time series leading up to the targets, we next asked how target onset affected the ongoing ITPC response. Informal observations by other researchers have suggested that ITPC may either increase or decrease when a visual target appears within a flickering display (Andreas Keil, personal communication, September 2022). We found this to be the case in our data as well, despite the fact that our grating targets were additively combined with the SSVER stimulus and flickered in phase with it. Therefore, we first characterized the change in ITPC after each target, which we call the "target-evoked ITPC response", for each observer.

Across observers, the ITPC amplitude changed briefly following each target, with a peak around 130 ms (**Figure 6**). For each experimental session for each observer, we used an automated peak-finding algorithm to identify peaks in the ITPC time series following the targets. For 4/10 observers the peak value of the target-evoked ITPC response was greater than the adjacent values (upward peaks), for 5/10 observers it was less than the adjacent values (downward peaks), and for one observer, the peak-finding algorithm was unable to identify peaks during the expected time windows. (We did not consider this observer further in the post-target ITPC analyses.) Individual peak times were consistent across observers, regardless of the direction of the peaks (T1 peak time mean = 1183 ms, SD = 28 ms; T2 peak time mean = 1479 ms, SD = 30 ms) (**Supplementary Figure 2**). The direction of the peaks was the same across sessions for each observer, indicating that the interaction of the targets with the ongoing SSVER signal was observer-specific. Inspection of the MEG time series for observers with upward vs. downward target-evoked ITPC responses suggested that upward responses reflected an enhancement of the ongoing SSVER signal when the target was superimposed on the flickering noise, whereas downward responses reflected a disruption of the SSVER signal by target-evoked activity (**Figure 6**).

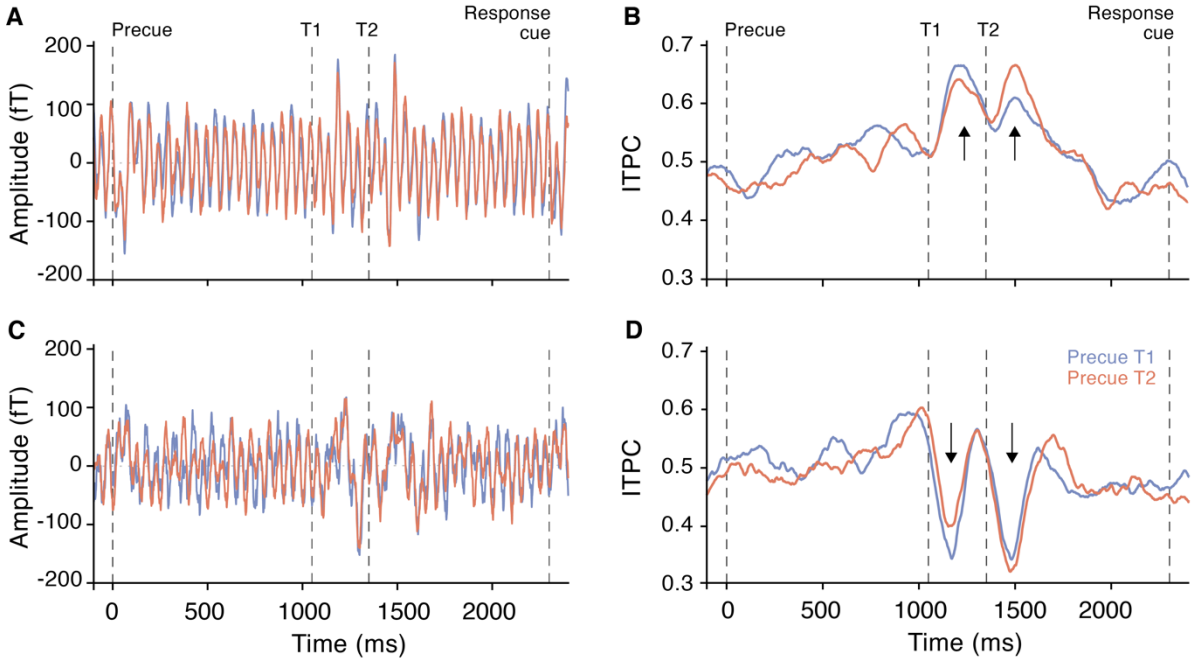

Figure 6. ITPC time series and evoked ITPC response peaks for example observers. (**A,C**) Evoked time series and (**B,D**) 20 Hz ITPC time series for two example observers. Target-evoked ITPC responses increased for some observers (e.g., top row) and decreased for others (e.g., bottom row). Blue = precue T1, red = precue T2. Arrows show the directions of the target-evoked ITPC responses.

To our knowledge, there is no accepted explanation for the observer-specific directionality of target-evoked ITPC responses. We investigated whether the direction of the target-evoked ITPC response for each observer could be predicted by a variety of factors, including demographics (age, gender, handedness), behavior (*d'*, RT), and other properties of the ITPC signal (topography, baseline value, peak timing, precue-to-T1 slope), but found no association with any of these factors (**Supplementary Table 1**, **Supplementary Figure 3**). Nevertheless, the target-evoked ITPC responses were a highly reliable measure of target-related activity, so we proceeded to ask whether they depended on voluntary temporal attention.

Temporal attention transiently affected the target-evoked ITPC response

We asked how temporal attention affected the magnitude of the target-evoked ITPC response. To be able to combine data from observers with upward and downward peaks, we first normalized the data from each observer by subtracting the value of a pre-stimulus baseline and then sign-flipping the resulting time series so that all observers' target-evoked ITPC peaks pointed upward (see Methods). As expected, the group average normalized ITPC time series has clear upward peaks after each target (**Figure 7A**).

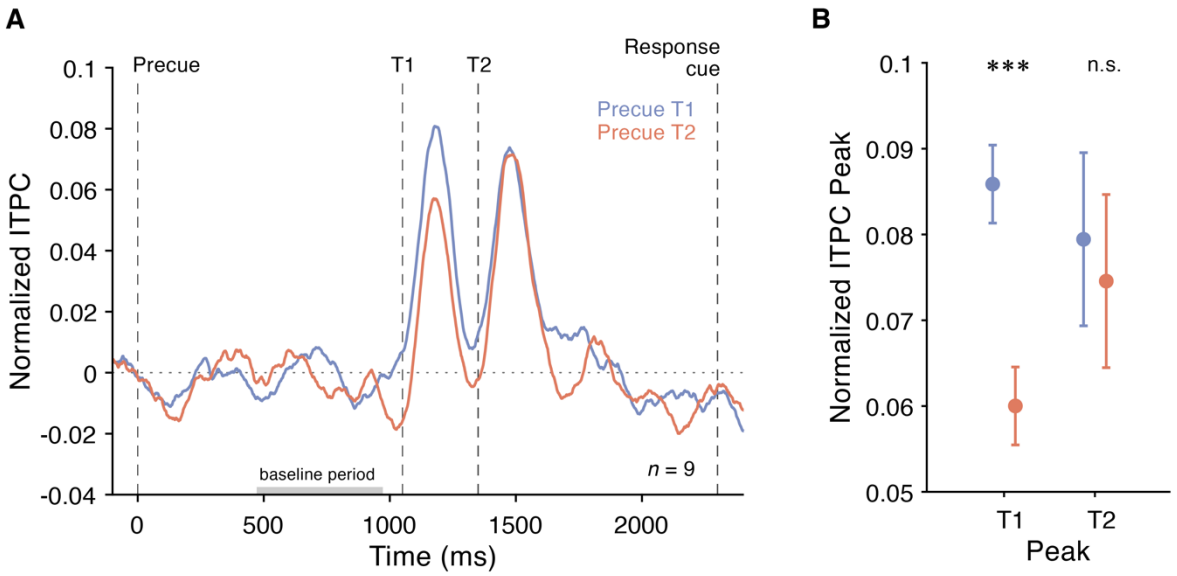

Figure 7. Group normalized ITPC. (**A**) Group normalized 20 Hz ITPC time series for each precue condition. Gray bar indicates the 500 ms baseline period used for normalization. (**B**) Effect of temporal attention on normalized target-evoked ITPC responses measured at individual observer peak times. Temporal attention increased the target-evoked ITPC response for T1. Error bars indicate ±1 SED.

The magnitude of the target-evoked ITPC response to T1 was larger when T1 was precued than when T2 was precued. To quantify the magnitude of this difference, we measured the peak of the normalized target-evoked ITPC response for each individual observer for the two precue types (see Methods). We found that temporal attention increased the target-evoked ITPC response to T1 ($F(1,8) = 32.34$, $p = 0.0004$, $\eta_G^2 = 0.23$; precue T1: mean = 0.086, SD = 0.088; precue T2: mean = 0.060, SD = 0.083 (**Figure 7B**). We found no significant effect of the precue on the response to T2 ($F(1,8) = 0.23$, $p = 0.64$, $\eta_G^2 = 0.005$; precue T1: mean = 0.079, SD = 0.086; precue T2: mean = 0.075, SD = 0.088). The presence of an effect of the precue for T1 and absence for T2 was reflected in a significant interaction of target and validity ($F(1,8) = 7.17$, $p = 0.028$, $\eta_G^2 = 0.055$). See **Supplementary Table 2** for all ANOVA results for the target-evoked response analyses.

We further investigated the effect of the precue on other measures of the evoked response to the targets. At the same peak times, trial-average normalized SSVER power behaved similarly to ITPC, whereas single-trial normalized 20 Hz power was unrelated to precue validity (**Supplementary Table 2**). Specifically, temporal attention increased the trial-average normalized SSVER power in response to T1 ($F(1,8) = 5.80$, $p = 0.043$, $\eta_G^2 = 0.11$; precue T1: mean = 560 fT^2, SD = 560 fT^2; precue T2 mean = 407 fT^2, SD = 454 fT^2) but not T2 ($F(1,8) = 0.22$, $p = 0.65$, $\eta_G^2 = 0.0026$; precue T1: mean = 406 fT^2, SD = 487 fT^2; precue T2 mean = 377 fT^2, SD = 497 fT^2, **Supplementary Figure 1H**). Single-trial normalized 20 Hz power, in contrast, showed no effect of precue for either target ($F(1,8) < 2.05$, $p > 0.19$, **Supplementary Figure 1I**), demonstrating that the change in ITPC was not driven by a change in 20 Hz power regardless of phase. Finally, we confirmed that the ITPC effect for T1 was specific to 20 Hz (**Supplementary Figure 4**). Therefore, directing temporal attention to the first target changed the steady-state response to that target in a transient fashion.

Discussion

Temporal expectation and temporal attention both affected cortical response reliability in anticipation of the target stimuli. Temporal expectation, reflecting the predictable timing of the target stimuli, was associated with a slow, ramping increase in visual response reliability as target onset approached. Temporal attention, reflecting the task relevance of targets at specific times, changed the rate of pre-target ramping and led to transient changes in target-evoked responses.

Effects of temporal expectation

Previous studies of temporal expectation have found anticipatory ramps in EEG voltage known as the contingent negative variation (CNV), often when a speeded response to a target was required (Amit et al., 2019; Breska and Ivry, 2020; Correa et al., 2005; Mento et al., 2015; Miniussi et al., 1999; Walter et al., 1964). The CNV is usually associated with response preparation or interval timing (Ng et al., 2011) and has been localized to frontal and parietal areas (Mento, 2017). Ramping activity in motor and parietal areas has also been observed leading up to timed movements (Maimon and Assad, 2006; Mita et al., 2009). Here instead we found expectation-related ramping activity in stimulus-specific sensory responses. Further, whereas the CNV and previously observed ramping signals reflected voltage amplitude or neuronal firing rate, here we found a ramping increase in ITPC, which reflects the reliability with which the SSVER stimulus drives neural responses.

A few studies have found expectation-related modulations of visual areas. In two studies, temporal expectations interacted with spatial (Ghose and Maunsell, 2002) or feature-based (Warren et al., 2014) attention, such that attentional modulation of visual responses in V4 or V1, respectively, was larger at times when targets were expected. Another study found that temporal expectations led to alpha reductions and gamma increases in macaque V1 in response to irrelevant gratings (Lima et al., 2011). Gamma ramped up over the course of ~1 s before the expected target time. Here we found a ramping enhancement of stimulus-driven ITPC. All of these previous studies employed speeded change detection tasks, leaving open the possibility that the cortical modulations were associated with response preparation or changes in response criterion. In our task, responses were not made until after the response cue, ruling out this possibility.

One previous study has investigated temporal expectation using SSVER, with mixed results (Mora-Cortes et al., 2017). This study found post-target increases in SSVER amplitude for predictable vs. unpredictable stimuli for some flicker frequencies, but reversed effects at other flicker frequencies and in the harmonics, with variable dynamics. No increase in SSVER amplitude in advance of a predictable target time emerged. However, the SSVER stimulus had no spatial overlap with the target location, so any expectation-related modulation specific to the target location would not have been visible in the SSVER signal.

SSVER studies of spatial attention sustained across seconds have reported SSVER amplitudes that are relatively constant across a trial (Kashiwase et al., 2012; Kim et al., 2007). This finding suggests that the ramping pattern we observed is specific to situations when the observer has a temporal expectation of a predictable target onset. Future studies using time-resolved SSVER should further investigate what kinds of anticipatory and preparatory processes drive ramping increases in cortical response reliability.

Effects of temporal attention

Critically, as in our previous studies (Denison et al., 2021, 2019, 2017; Fernández et al., 2019), our task allowed us to measure specific effects of temporal attention to task-relevant time points, over and above the effects of temporal expectation due to predictable stimulus timing. Our

normalization model of dynamic attention predicts that temporal attention will modulate neural responses at a sensory level (Denison et al., 2021). Based on fits to psychophysical data, the model also predicts that the effects of temporal attention on neural gain will be transient and roughly coincident with the sensory responses.

The current data are consistent with both model predictions: sensory modulation by temporal attention and modulation at a transient timescale. Specifically, the model predicts a change in gain at the neuronal level, which requires a linking hypothesis to make predictions for MEG measures. Gain increases would increase the probability or rate of neuronal spiking in response to each stimulus flicker, which in turn would be expected to lead to more reliable population responses to the SSVER stimulus across trials and thus higher ITPC. However, such a mechanism also might be expected to increase single-trial power, which we did not observe. One possible resolution is that gain increases did occur but that stimulus-driven 20 Hz activity entrained or otherwise interacted with ongoing endogenous (non-phase locked) 20 Hz power, which would be consistent with the low SNR we observed for single-trial power at 20 Hz. Alternatively, it could be the case that changes in ITPC arose from a mechanism other than gain changes, such as more consistent timing of stimulus-driven responses without changes in neuronal response amplitude. Invasive recordings and perhaps modeling efforts could distinguish between these possibilities.

This linking hypothesis between gain increases at the neuronal level and ITPC increases in the SSVER can account for the pre-target effects of attention and expectation we observed, as well as post-target effects for those observers showing an increase in the ITPC evoked response following each target. However, as we discuss below, ITPC evoked-response decreases appear to arise from observer-specific interactions between the ongoing SSVER and target-evoked responses and are thus not predictable from the normalization model of dynamic attention, which does not include specific biophysical structure.

The current results also reveal an effect of temporal attention not predicted by the model: a modulation of the rate of anticipatory ramping in sensory reliability over the 1 s leading up to stimulus onset. It is not surprising that the model did not predict anticipatory ramping, because behavioral data alone cannot reveal anticipatory dynamics; future versions of the model should incorporate these new experimental findings. Interestingly, an overall effect of temporal expectation that is modulated by temporal attention is similar to the pattern we have observed for microsaccades, which also provide continuous measures of anticipatory processes (Denison et al., 2019).

Effects of temporal cueing on early evoked visual responses have also been observed in previous studies, which measured changes in EEG amplitude (Correa et al., 2006) or multi-unit activity in IT (Anderson and Sheinberg, 2008) within 100 ms post-stimulus. However, these studies could not assess whether this sensory modulation was truly transient, as there was no visual stimulation (and thus no stimulus-driven activity) before or after the targets. Moreover, in these studies only a single target was presented on each trial, so temporal attention and expectation could not be disentangled.

Our two-target design allowed us to measure how temporal attention affected evoked responses to both T1 and T2 and to distinguish those effects from temporal expectation. In experimental designs with one target occurring at an expected or unexpected time, observers can reorient to a later time if a target does not appear at an earlier time (Coull and Nobre, 1998; Nobre and Ede, 2018). This reorienting strategy is not possible with two targets and a response cue, because observers must wait for the response cue to find out which target to report. Here we found that

temporal attention affected the evoked ITPC response only to T1 and not to T2. We also found only a marginal effect (statistical trend) of temporal attention on T2 *d'*, so it may be that the effect of temporal attention on target processing was generally weaker for T2 than T1. Another possibility, albeit speculative, is that because of the directionality of time, the neural mechanisms of temporal attention differ for T1 and T2. For example, if the pre-target ramping we observed before T1 is causally related to the neural response to the target, this mechanism would be able to impact T1 but not T2. It may be that at early sensory stages, changing the relative responses to the two targets by modulating T1 alone is sufficient to bias downstream competition between the two target representations and produce attentional tradeoffs in behavior. In our data, the ITPC response to T2 is lower than the T1 response on precue T1 trials but higher on precue T2 trials, consistent with a relative modulation of target responses by attention.

A limitation of our approach of characterizing the ramping activity with linear fits is that the ITPC ramps may not be strictly linear. This possibility was hinted at by the group ITPC time series for each precue condition, which looked like they could have periodic modulations. Alternatively, apparent deviations from linearity could be due to noise. In an exploratory analysis, we investigated possible periodicities in the precue-to-T1 interval but failed to find reliable evidence for periodic modulations across observers, leading us to use a simple linear fit. The present results, then, indicate that there is a difference between temporal attention conditions in the linear component of the SSVER signal as the presentation of the first target approaches.

ITPC as a measure of cortical response reliability

We quantified cortical response reliability to periodic visual stimulation using ITPC, a measure of phase consistency across trials. Many previous studies using steady state methods have measured the strength of sensory responses using the power of the SSVER signal (at the stimulus frequency) computed from the average time series across trials, i.e., the trial-average SSVER power (Andersen and Müller, 2010; Morgan et al., 1996; Müller et al., 1997). Here we focused on ITPC because it is more specific than the trial-average power, which depends on both phase consistency across trials (ITPC) and power at the stimulus frequency on single trials. Studies that have pulled apart ITPC and single-trial power found that trial-average SSVER power is mainly driven by ITPC (Ding et al., 2006; Kashiwase et al., 2012; Kim et al., 2007), with ~70% of the signal variance explained by ITPC and only ~10% explained by single-trial power (Moratti et al., 2007). Consistent with these observations, we found that trial-average power was similar to ITPC and that temporal attention and expectation affected ITPC but not single-trial power at the SSVER frequency.

Spatial attention increases ITPC, which has been interpreted as arising from an increase in the synchronization of neurons (Kashiwase et al., 2012; Kim et al., 2007). It is important to distinguish synchronization of a neural population within a trial, which would be expected to increase single-trial SSVER power, from neural synchronization across trials, which would be expected to increase ITPC. Here we adopt a descriptive approach, interpreting ITPC as a measure of response reliability to the visual flicker: a stimulus that more reliably drives the neural response will yield a higher phase coherence across trials.

Individual differences in responses to a target embedded in the steady state stimulus

Embedding targets in SSVER streams allows the investigation of both anticipatory and target-related dynamics. Here we found that individual observer analysis is critical to investigate target-related dynamics. Specifically, we observed that embedded, brief targets presented in phase with the SSVER flicker interacted differently with the ongoing SSVER signal for different observers. Some observers showed increased ITPC following target presentation due to an enhancement of

the SSVER response whereas some showed decreased ITPC due to a disruption of the periodic signal.

Few studies have embedded targets in SSVER stimuli. Such studies have observed decreases in the SSVER group average (Campagnoli et al., 2019; Eidelman-Rothman et al., 2019; Müller et al., 2008), but individual differences were not reported in these studies. In a study of emotion processing, decreases in SSVER following a transient target have been interpreted as a withdrawal of attentional resources to the SSVER stimulus (Müller et al., 2008). In the current study, however, the flickering noise patch completely overlapped the target in feature space (orientation and spatial frequency) as well as in physical space. Moreover the attentional benefit was similar regardless of whether ITPC increased or decreased following target presentation, ruling out the possibility that the evoked decreases we observed were related to a withdrawal of attention from the SSVER stimulus in our study.

Because the interaction between the targets and SSVER were highly consistent across sessions for each individual, we could characterize the impact of the target on the SSVER signal for each observer and show that temporal attention increases this impact. However, the interpretation of the directionality of target-evoked ITPC responses, regardless of attention, remains a challenge in the field. It is recognized that ITPC around the time of evoked responses can depend on the amplitude and latency of the evoked responses (Diepen and Mazaheri, 2018), but it is unclear what mechanism could cause a directional change. Future research should investigate the mechanism underlying individual differences in the interaction of the target response and the ongoing SSVER.

Conclusions

By measuring how voluntary attention to points in time continuously impacts the reliability of cortical responses to visual stimulation, we revealed two complementary neural mechanisms of temporal attention and expectation: (1) a slow, pre-target ramping of visual cortical ITPC that anticipated predictable target times and was modulated by which time point was to be attended, and (2) a transient, post-target increase of the evoked ITPC response to targets at attended time points, which was specific to the first target. This transient modulation changed the relative strengths of the two target responses as a function of attention. These findings help reconcile previous neural findings showing expectation-related ramps in fronto-parietal areas and theoretical work predicting transient post-target changes in visual responses. They suggest that the documented effects of temporal attention on perceptual sensitivity at the behavioral level are mediated by changes in neural reliability at the level of visual cortex. Moreover, they chart and differentiate the full time course of these expectation- and attention-related dynamics.

Methods

Observers

Ten observers (5 females), ages 24-35 years (M = 28.5 years, SD = 4.2 years) participated, including authors R.N.D and K.T. The sample size was similar to previous temporal attention studies that measured accuracy (Davranche et al., 2011; Denison et al., 2017; Fernández et al., 2019) and to several studies on spatial attention (Anton-Erxleben et al., 2012; Fernández and Carrasco, 2020; Jigo and Carrasco, 2020). All observers provided informed consent, and the University Committee on Activities involving Human Subjects at New York University approved the experimental protocols. All observers had normal or corrected-to-normal vision.

Stimuli

Stimuli were generated on an Apple iMac using MATLAB and Psychophysics Toolbox (Brainard, 1997; Pelli, 1997) and were displayed using a gamma-corrected InFocus LP850 projector (Texas Instruments, Warren, NJ) with a resolution of 1024 x 768 pixels and a refresh rate of 60 Hz. Stimuli were projected via a mirror onto a translucent screen at a viewing distance of 42 cm. Stimulus timing accuracy was confirmed with photodiode measurements. Stimuli were presented on a medium gray background (206 cd/m^2). A central fixation circle subtended 0.15° visual angle.

SSVER stimulus. Throughout the trial, a 20 Hz contrast-reversing flickering noise patch was presented foveally, with the fixation circle overlaid. The noise patch was 4° in diameter with a blurred outer edge subtending 0.4°, fading to the background gray. To create the noise patch, pixel noise was generated from a normal distribution then bandpass filtered in both orientation and spatial frequency around target values: in orientation 0° ± 5° and 90° ± 5° forming a vertical and horizontal crosshatch pattern, and in spatial frequency 1.5 cpd ± 1 octave. A new noise patch was randomly generated on each trial and then flickered throughout the trial with a duty cycle of 33% (1 frame of the original noise image in alternation with 2 frames of the contrast-reversed image). The contrast of the SSVER stimulus was adjusted to ensure high visibility of the target stimuli while still producing a clear SSVER signal (40-55% noise patch contrast across observers).

Targets. Visual targets were 1.5 cpd sinusoidal gratings of 4° in diameter with a blurred outer edge subtending 0.4°. Targets were also presented foveally and were added pixelwise to the noise patch stimulus. To match the temporal frequency of the targets to the SSVER stimulus, the targets were also contrast-reversed for 2 cycles at 20 Hz, in phase with the noise patch flicker, for a total target duration of 100 ms. Target grating contrast was adjusted so that, when added to the noise patch, the total contrast was 100% (grating contrast 45-60% across observers).

Cues. Auditory cues were pure sine wave tones 100 ms in duration (with 10 ms cosine amplitude modulation ramps at onset and offset) presented through earbuds at a comfortable volume. There were two possible auditory cue tones, one high-pitched (1046.5 Hz, C6) and one low-pitched (440 Hz, A4).

Experimental procedure

All observers participated in two 2-hour MEG sessions on separate days, on average 3.6 days apart. Each session included 12 experimental blocks approximately 6 minutes each in duration. Observers took breaks between blocks and pressed a button to indicate their readiness for the next block.

Task. On each trial, observers were asked to discriminate the orientation of one of two grating targets (**Figure 1**). The two targets (T1 and T2) were each presented for 100 ms, separated by a stimulus onset asynchrony (SOA) of 300 ms, based on previous psychophysical studies (Denison et al., 2021, 2017; Fernández et al., 2019). Each target was tilted slightly clockwise (CW) or counterclockwise (CCW) from either the vertical or horizontal axis, with independent tilts and axes for T1 and T2. Both vertical and horizontal axes were used to reduce the number of trials on which the two stimuli were identical and discourage observers from adopting a strategy of judging whether the stimuli were the same or different to aid in discrimination. An auditory precue 1,050 ms before the first target instructed observers to attend to the first or the second target (high tone: attend T1; low tone: attend T2). An auditory response cue 950 ms after T2 indicated which of the two targets' tilt to report (high tone: report T1; low tone: report T2). Observers pressed one of two buttons to indicate whether the tilt was CW or CCW relative to the main axis within a 1600 ms response window. The response cue matched the precue on 75% of the trials (valid trials) and mismatched the precue on the remaining 25% (invalid trials). At the end of each trial, feedback

was provided by a change in color of the fixation circle (green: correct; red: incorrect; blue: response timeout). At the end of each block, performance accuracy (percent correct) was displayed. The timing of auditory and visual events was the same on every trial. From trial to trial, the allocation of temporal attention varied (depending on the precue), and the response selection varied (depending on the response cue).

So that only the precue would provide predictive timing information about the target onsets, and to allow time for the SSVER signal to stabilize before any trial events occurred, the interval between the SSVER onset and the precue was jittered from 500 to 1500 ms in steps of 200 ms. Between each trial, an inter-trial interval of 1500 ms was presented, during which only the fixation circle appeared on a gray background. Observers were encouraged to blink during this period. The fixation circle turned black at the start of the ITI, turned white 500 ms before the SSVER onset to indicate that the trial was about to begin, and remained white throughout the trial until the response feedback was provided.

Each session consisted of 12 blocks of 41 trials each with all combinations of cue type (valid: 75%, invalid: 25%), probed target (T1, T2), target tilt (CW, CCW; independent for T1 and T2), and target axis (horizontal, vertical; independent for T1 and T2) in a randomly shuffled order. To reduce adaptation to the SSVER stimulus, every fifth trial was a blank trial, with an additional blank trial at the beginning of each block. This procedure yielded a total of 768 temporal attention trials per observer across the two sessions.

Training and thresholding. Prior to MEG, observers completed at least one session of training to familiarize them with the task and to determine their orientation tilt thresholds. During the training session, a chin-and-head rest was used to hold head position and viewing distance constant. Stimuli were displayed on a gamma-corrected Sony Trinitron G520 CRT monitor with a refresh rate of 60 Hz at a viewing distance of 57 cm. A 3-up-1-down staircase procedure was used to estimate each observer's tilt threshold to achieve ~79% accuracy across all trials. Threshold tilts ranged from 1.5-5°.

Eyetracking. Eye position was recorded using an EyeLink 1000 eye tracker (SR Research) with a sampling rate of 1000 Hz. Raw gaze positions were converted into degrees of visual angle using the five-point-grid calibration, which was performed at the start of each MEG session.

MEG recording. Data were recorded continuously in each block with a 157-channel axial gradiometer system (Kanazawa Institute of Technology, Kanazawa, Japan) in the KIT/NYU facility at New York University. The magnetic fields were sampled at 1000 Hz with online DC filtering and a 200 Hz high-pass filter. Three orthogonally-oriented reference magnetometers placed approximately 20 cm away from the recording array recorded environmental noise.

Before recording, each observer's head shape was digitized with a handheld FastSCAN laser scanner (Polhemus, VT, USA). Digital markers were placed on the forehead, nasion, and left and right tragus and peri-auricular points. To record marker locations with respect to the MEG channels, electrodes were placed on five of the locations identified by the digital markers (three points on the forehead and left and right peri-auricular points), and marker locations were measured at the beginning and end of the MEG recording session.

Data analysis

Preprocessing. Data was preprocessed in MATLAB using the FieldTrip toolbox for EEG/MEG-analysis (Oostenveld et al., 2011). Environmental noise was removed from the data by regressing signals recorded from three orthogonally oriented magnetometers against the recorded data.

MEG channels in which there was no signal or excessive noise were interpolated from neighboring channels (the number of interpolated channels per recorded session ranged from 2 to 16 (1.3-10.2%), mean = 3.9 (2.5%), SD = 3.0. Trials were manually inspected and rejected for blinks and other artifacts. The number of rejected trials per session ranged from 26 to 73 (5.3-14.8%), mean = 45.4 (9.2%), SD = 14.3.

Channel selection. We selected visually responsive channels as the five channels per session with the strongest 20 Hz trial-average SSVER power. Topographies confirmed selected channels were in the posterior part of the head.

SSVER analysis. For the SSVER analyses, trials were epoched from 1500 ms before to 5200 ms after the precue. Time-frequency representations of the data were computed using wavelet convolution with the FieldTrip toolbox. For the 20 Hz SSVER frequency, Morlet wavelets had 8 cycles (127 ms temporal resolution, 5 Hz spectral resolution). For full time-frequency spectra, frequency was sampled every 1 Hz from 1-50 Hz, time was sampled every 10 ms, wavelets were tapered with Hanning windows, and the time windows scaled with frequency according to 10 s divided by the frequency.

Trial-average power. Trial-average power quantifies the power of a periodic signal that is phase-locked across trials and so survives averaging across trials. This measure has been commonly used in the SSVER literature (Morgan et al., 1996; Müller et al., 1998b, 1998a; Norcia et al., 2015). To calculate the trial-average power, the time series of all trials (or all trials in a given experimental condition) were first averaged together, giving the mean time series across trials. Time-frequency analysis was then performed on this single time series to calculate the power across time at a frequency of interest. Trial-average power depends on two factors: single-trial power and ITPC.

Single-trial power. Single-trial power quantifies the power of a periodic signal present on individual trials. To calculate the single-trial power, time-frequency analysis was performed on each individual trial, and these time-frequency representations were then averaged together across trials. This procedure preserves oscillatory activity that is not phase-locked across trials but relies on having sufficient signal-to-noise at the single trial level to measure the periodic signal.

ITPC. Inter-trial phase coherence (ITPC) quantifies the phase alignment of a periodic signal across trials. The measure ranges from 0 (no phase alignment) to 1 (perfect phase alignment) (Lachaux et al., 1999). To calculate ITPC, time-frequency analysis was performed on each individual trial, returning estimates of the instantaneous phase angle at each point in time for a frequency of interest. The following standard formula was then used to calculate the alignment of these phase angles across trials, providing an estimate of ITPC:

$$ITPC_{tf} = \frac{1}{N}\left|\sum_{n=1}^{N} e^{i\phi_{tf}}\right|$$

where ϕ_{tf} is the instantaneous phase angle in radians at a time point t and frequency f for each trial $n \in [1,\ldots,N]$.

Slope analysis. To quantify the pre-target ITPC ramping rate for individual observers, we fit lines to the ITPC time series in the time window between the precue and first target. In all trials, a predictable interval of 1.05 s elapsed between the onset of the precue and the onset of T1, so observers could form an expectation about the timing of T1 onset. To prevent T1 from influencing ITPC measurements of pre-target activity due to the temporal bandwidth of the wavelet, we set a cushion before T1 based on the group average ITPC time series across all trials. The start of the cushion was the inflection point 80 ms before T1 when ITPC began to sharply decrease due to the T1 response. Thus the precue-to-T1 window was defined as the onset of the precue to 80 ms before T1.

To assess the overall effect of expectation on ITPC in this precue-to-T1 period, we fit lines to the ITPC time series calculated from all trials. To assess the effect of temporal attention, we fit lines to ITPC time series calculated from trials for each precue condition separately. In all cases, we fit lines for each observer and session and then statistically assessed the slope parameters from these fits.

We also investigated whether there was any basis in the data for assessing periodic activity in the precue-to-T1 period, in addition to a linear ramp. To do so, we performed FFTs of the ITPC time series in this period, both across all trials and split up by precue condition, and assessed the resulting frequency distributions across observers using non-parametric tests. However, we did not find the power in any specific frequency bin (1-20 Hz, 1 Hz resolution) to differ from the null distribution after correcting for multiple comparisons.

Peak analysis. To quantify the evoked ITPC response for individual observers, we estimated the latency, direction, and amplitude of the most prominent deflection in the 20 Hz ITPC following each target, which we refer to as a “peak”. As ITPC data in the selected visual channels was highly consistent across sessions for a given observer, we identified peak times for each observer using the ITPC time series averaged across the two sessions. To find the peaks, we applied the MATLAB algorithm *findpeaks.m* to the time window 0 ms to 600 ms after T1 onset, which captured the evoked ITPC responses to both T1 and T2.

All observers but one had two peaks that were either upward or downward during this window. The observer without an identifiable pair of peaks was not considered further in the peak analysis. Two observers had both upward peaks and downward peaks during the window, so for these observers we selected the pair of peaks whose timing was best aligned with the peaks of the other observers. The direction of the pair of peaks identified by this algorithm determined the classification of an observer as having either upward or downward peaks.

We next assessed the effect of attention on the magnitude of the ITPC peaks, regardless of their direction. To combine evoked ITPC data across observers for this analysis, we first normalized the data so that peaks for all observers pointed upward. To do so, we measured a baseline ITPC value for each observer and session in the window 470-970 ms after the precue (a 500 ms window before target onset, excluding the 80 ms cushion before T1, see “Slope analysis”). We then subtracted that baseline value from the time series, and for observers with downward peaks, reversed the sign:

$$ITPC_{\text{normalized}} = (ITPC - baseline) * s$$

where s = 1 for observers with upward peaks and -1 for observers with downward peaks. This procedure allowed all evoked ITPC peaks to point upward while preserving all other features of the time series.

Finally, to quantify the ITPC magnitude at the peak times, for each observer, session, and precue condition, we took the mean normalized ITPC value in a 100 ms window centered on each peak time (i.e., following each target). Equivalent peak analyses were performed for trial-average 20 Hz power and single-trial 20 Hz power using the same peak times and normalization procedure.

Statistical analysis. The effects of temporal attention on behavior (*d'* and RT and MEG time series (slopes and peak values) were assessed using repeated measures ANOVAs via the *ezANOVA* package in R. For behavioral data, the within-subject factors were session, target, and validity (valid or invalid, with respect to the match between the precue and response cue), with session as an observed factor. For MEG slope analyses, within-subject factors were session and precue (precue T1 or precue T2), with session as an observed factor. For MEG peak analyses, within-subject factors were session, target, and attention (attended or unattended, with respect to the precue type, referenced to each target), with session as an observed factor. Planned ANOVAs were also conducted for each target separately.

To assess the effect of the precue on the full time series or time-frequency spectrum, we used a non-parametric test with cluster correction (Maris and Oostenveld, 2007). This involved a two-step procedure using data averaged across sessions for each observer. In the first step, paired t-tests were performed at each time point or time-frequency bin (henceforth, "bin" for both) comparing precue T1 to precue T2 condition values. This operation yielded t-statistics for each bin for the empirical data. Contiguous bins passing the $p < 0.05$ threshold were considered to form a cluster, and a statistic was generated for each cluster by taking the sum of the t-values for bins within the cluster. The largest statistic out of all clusters was considered to be the maximum cluster statistic for the empirical data. Next, null distributions of the maximum cluster statistic were constructed by shuffling the labels for the precue conditions, computing the maximum cluster statistic for the shuffled data, and repeating this process 1000 times. Significance levels for the empirical data was determined by comparing the value of the maximum cluster statistic to the null distribution.

Acknowledgements

We thank Sirui Liu and Luis Ramirez for assistance with early versions of the experiment. We thank Hsin-Hung Li, Amit Yashar, and members of the Carrasco and Denison Labs for helpful comments. We thank Jeffrey Walker at the NYU MEG lab for technical assistance. This research was supported by National Institutes of Health National Eye Institute R01 EY019693 to M.C., F32 EY025533 to R.N.D. and T32 EY007136 to NYU, by Department of Defense NDSEG to K.T., and by funding from Boston University to R.N.D.

References

Amit R, Abeles D, Carrasco M, Yuval-Greenberg S. 2019. Oculomotor inhibition reflects temporal expectations. *Neuroimage* 184:279–292. doi:10.1016/j.neuroimage.2018.09.026

Andersen SK, Müller MM. 2010. Behavioral performance follows the time course of neural facilitation and suppression during cued shifts of feature-selective attention. *Proc National Acad Sci* 107:13878–13882. doi:10.1073/pnas.1002436107

Anderson B, Sheinberg DL. 2008. Effects of temporal context and temporal expectancy on neural activity in inferior temporal cortex. *Neuropsychologia* 46:947–957. doi:10.1016/j.neuropsychologia.2007.11.025

Anton-Erxleben K, Herrmann K, Carrasco M. 2012. Independent effects of adaptation and attention on perceived speed. *Psychol Sci* 24:150–159. doi:10.1177/0956797612449178

Bang JW, Rahnev D. 2017. Stimulus expectation alters decision criterion but not sensory signal in perceptual decision making. *Sci Rep-uk* 7:17072. doi:10.1038/s41598-017-16885-2

Brainard DH. 1997. The psychophysics toolbox. *Spatial Vision* 10:433–436. doi:10.1163/156856897x00357

Breska A, Ivry RB. 2020. Context-specific control over the neural dynamics of temporal attention by the human cerebellum. *Sci Adv* 6:eabb1141. doi:10.1126/sciadv.abb1141

Campagnoli RR, Wieser MJ, Gruss LF, Boylan MR, McTeague LM, Keil A. 2019. How the visual brain detects emotional changes in facial expressions: Evidence from driven and intrinsic brain oscillations. *Cortex* 111:35–50. doi:10.1016/j.cortex.2018.10.006

Cheadle S, Egner T, Wyart V, Wu C, Summerfield C. 2015. Feature expectation heightens visual sensitivity during fine orientation discrimination. *J Vision* 15:14. doi:10.1167/15.14.14

Correa Á, Lupiáñez J, Madrid E, Tudela P. 2006. Temporal attention enhances early visual processing: A review and new evidence from event-related potentials. *Brain Res* 1076:116–128. doi:10.1016/j.brainres.2005.11.074

Correa Á, Lupiáñez J, Tudela P. 2005. Attentional preparation based on temporal expectancy modulates processing at the perceptual level. *Psychon B Rev* 12:328–334. doi:10.3758/bf03196380

Coull JT, Nobre AC. 1998. Where and when to pay attention: The neural systems for directing attention to spatial locations and to time intervals as revealed by both PET and fMRI. *J Neurosci* 18:7426–7435. doi:10.1523/jneurosci.18-18-07426.1998

Davranche K, Nazarian B, Vidal F, Coull J. 2011. Orienting attention in time activates left intraparietal sulcus for both perceptual and motor task goals. *J Cognitive Neurosci* 23:3318–3330. doi:10.1162/jocn_a_00030

Denison RN, Carrasco M, Heeger DJ. 2021. A dynamic normalization model of temporal attention. *Nat Hum Behav* 1–12. doi:10.1038/s41562-021-01129-1

Denison RN, Heeger DJ, Carrasco M. 2017. Attention flexibly trades off across points in time. *Psychon B Rev* 24:1142–1151. doi:10.3758/s13423-016-1216-1

Denison RN, Yuval-Greenberg S, Carrasco M. 2019. Directing voluntary temporal attention increases fixational stability. *J Neurosci* 39:353–363. doi:10.1523/jneurosci.1926-18.2018

Diepen RM van, Mazaheri A. 2018. The caveats of observing inter-trial phase-coherence in cognitive neuroscience. *Sci Rep-uk* 8:2990. doi:10.1038/s41598-018-20423-z

Ding J, Sperling G, Srinivasan R. 2006. Attentional modulation of SSVEP power depends on the network tagged by the flicker frequency. *Cereb Cortex* 16:1016–1029. doi:10.1093/cercor/bhj044

Eidelman-Rothman M, Ben-Simon E, Freche D, Keil A, Hendler T, Levit-Binnun N. 2019. Sleepless and desynchronized: Impaired inter trial phase coherence of steady-state potentials following sleep deprivation. *Neuroimage* 202:116055. doi:10.1016/j.neuroimage.2019.116055

Fernández A, Carrasco M. 2020. Extinguishing exogenous attention via transcranial magnetic stimulation. *Curr Biol* 30:4078-4084.e3. doi:10.1016/j.cub.2020.07.068

Fernández A, Denison RN, Carrasco M. 2019. Temporal attention improves perception similarly at foveal and parafoveal locations. *J Vision* 19:12–12. doi:10.1167/19.1.12

Finnerty GT, Shadlen MN, Jazayeri M, Nobre AC, Buonomano DV. 2015. Time in cortical circuits. *J Neurosci* 35:13912–13916. doi:10.1523/jneurosci.2654-15.2015

Ghose GM, Maunsell JHR. 2002. Attentional modulation in visual cortex depends on task timing. *Nature* 419:616–620. doi:10.1038/nature01057

Hillyard SA, Vogel EK, Luck SJ. 1998. Sensory gain control (amplification) as a mechanism of selective attention: electrophysiological and neuroimaging evidence. *Philosophical Transactions Royal Soc Lond Ser B Biological Sci* 353:1257–1270. doi:10.1098/rstb.1998.0281

Jigo M, Carrasco M. 2020. Differential impact of exogenous and endogenous attention on the contrast sensitivity function across eccentricity. *J Vision* 20:11. doi:10.1167/jov.20.6.11

Kashiwase Y, Matsumiya K, Kuriki I, Shioiri S. 2012. Time courses of attentional modulation in neural amplification and synchronization measured with steady-state visual-evoked potentials. *J Cognitive Neurosci* 24:1779–1793. doi:10.1162/jocn_a_00212

Kim YJ, Grabowecky M, Paller KA, Muthu K, Suzuki S. 2007. Attention induces synchronization-based response gain in steady-state visual evoked potentials. *Nat Neurosci* 10:117–125. doi:10.1038/nn1821

Kok P, Rahnev D, Jehee JFM, Lau HC, de Lange FP. 2012. Attention reverses the effect of prediction in silencing sensory signals. *Cereb Cortex* 22:2197–2206. doi:10.1093/cercor/bhr310

Lachaux J, Rodriguez E, Martinerie J, Varela FJ. 1999. Measuring phase synchrony in brain signals. *Hum Brain Mapp* 8:194–208. doi:10.1002/(sici)1097-0193(1999)8:4<194::aid-hbm4>3.0.co;2-c

Lange K, Röder B. 2006. Orienting attention to points in time improves stimulus processing both within and across modalities. *J Cognitive Neurosci* 18:715–729. doi:10.1162/jocn.2006.18.5.715

Leon MI, Shadlen MN. 2003. Representation of time by neurons in the posterior parietal cortex of the macaque. *Neuron* 38:317–327. doi:10.1016/s0896-6273(03)00185-5

Lima B, Singer W, Neuenschwander S. 2011. Gamma responses correlate with temporal expectation in monkey primary visual cortex. *J Neurosci* 31:15919–15931. doi:10.1523/jneurosci.0957-11.2011

Maimon G, Assad JA. 2006. A cognitive signal for the proactive timing of action in macaque LIP. *Nat Neurosci* 9:948–955. doi:10.1038/nn1716

Maris E, Oostenveld R. 2007. Nonparametric statistical testing of EEG- and MEG-data. *J Neurosci Meth* 164:177–190. doi:10.1016/j.jneumeth.2007.03.024

Mento G. 2017. The role of the P3 and CNV components in voluntary and automatic temporal orienting: A high spatial-resolution ERP study. *Neuropsychologia* 107:31–40. doi:10.1016/j.neuropsychologia.2017.10.037

Mento G, Tarantino V, Vallesi A, Bisiacchi PS. 2015. Spatiotemporal neurodynamics underlying internally and externally driven temporal prediction: A high spatial resolution ERP study. *J Cognitive Neurosci* 27:425–439. doi:10.1162/jocn_a_00715

Merchant H, Harrington DL, Meck WH. 2013. Neural basis of the perception and estimation of time. *Annu Rev Neurosci* 36:313–336. doi:10.1146/annurev-neuro-062012-170349

Miniussi C, Wilding EL, Coull JT, Nobre AC. 1999. Orienting attention in time: Modulation of brain potentials. *Brain* 122:1507–1518. doi:10.1093/brain/122.8.1507

Mita A, Mushiake H, Shima K, Matsuzaka Y, Tanji J. 2009. Interval time coding by neurons in the presupplementary and supplementary motor areas. *Nat Neurosci* 12:502–507. doi:10.1038/nn.2272

Mora-Cortes A, Ridderinkhof KR, Cohen MX. 2017. Evaluating the feasibility of the steady-state visual evoked potential (SSVEP) to study temporal attention. *Psychophysiology* 55:e13029. doi:10.1111/psyp.13029

Moratti S, Clementz BA, Gao Y, Ortiz T, Keil A. 2007. Neural mechanisms of evoked oscillations: Stability and interaction with transient events. *Hum Brain Mapp* 28:1318–1333. doi:10.1002/hbm.20342

Morgan ST, Hansen JC, Hillyard SA. 1996. Selective attention to stimulus location modulates the steady-state visual evoked potential. *Proc National Acad Sci* 93:4770–4774. doi:10.1073/pnas.93.10.4770

Müller MM, Andersen SK, Keil A. 2008. Time course of competition for visual processing resources between emotional pictures and foreground task. *Cereb Cortex* 18:1892–1899. doi:10.1093/cercor/bhm215

Müller MM, Picton TW, Valdes-Sosa P, Riera J, Teder-Sälejärvi WA, Hillyard SA. 1998a. Effects of spatial selective attention on the steady-state visual evoked potential in the 20–28 Hz range. *Cognitive Brain Res* 6:249–261. doi:10.1016/s0926-6410(97)00036-0

Müller MM, Teder W, Hillyard SA. 1997. Magnetoencephalographic recording of steadystate visual evoked cortical activity. *Brain Topogr* 9:163–168. doi:10.1007/bf01190385

Müller MM, Teder-Sälejärvi W, Hillyard SA. 1998b. The time course of cortical facilitation during cued shifts of spatial attention. *Nat Neurosci* 1:631–634. doi:10.1038/2865

Ng KK, Tobin S, Penney TB. 2011. Temporal accumulation and decision processes in the duration bisection task revealed by contingent negative variation. *Frontiers Integr Neurosci* 5:77. doi:10.3389/fnint.2011.00077

Nobre AC, Ede F van. 2018. Anticipated moments: Temporal structure in attention. *Nat Rev Neurosci* 19:34–48. doi:10.1038/nrn.2017.141

Norcia AM, Appelbaum LG, Ales JM, Cottereau BR, Rossion B. 2015. The steady-state visual evoked potential in vision research: A review. *J Vision* 15:4. doi:10.1167/15.6.4

Oostenveld R, Fries P, Maris E, Schoffelen J-M. 2011. FieldTrip: Open source software for advanced analysis of MEG, EEG, and invasive electrophysiological data. *Comput Intel Neurosc* 2011:156869. doi:10.1155/2011/156869

Pelli DG. 1997. The VideoToolbox software for visual psychophysics: transforming numbers into movies. *Spatial Vision* 10:437–442. doi:10.1163/156856897x00366

Richter D, Ekman M, de Lange FP. 2018. Suppressed sensory response to predictable object stimuli throughout the ventral visual stream. *J Neurosci* 38:7452–7461. doi:10.1523/jneurosci.3421-17.2018

Rohenkohl G, Gould IC, Pessoa J, Nobre AC. 2014. Combining spatial and temporal expectations to improve visual perception. *J Vision* 14:8–8. doi:10.1167/14.4.8

Rungratsameetaweemana N, Serences JT. 2019. Dissociating the impact of attention and expectation on early sensory processing. *Curr Opin Psychology* 29:181–186. doi:10.1016/j.copsyc.2019.03.014

Samaha J, Bauer P, Cimaroli S, Postle BR. 2015. Top-down control of the phase of alpha-band oscillations as a mechanism for temporal prediction. *Proc National Acad Sci* 112:8439–8444. doi:10.1073/pnas.1503686112

Summerfield C, Egner T. 2016. Feature-based attention and feature-based expectation. *Trends Cogn Sci* 20:401–404. doi:10.1016/j.tics.2016.03.008

Summerfield C, Egner T. 2009. Expectation (and attention) in visual cognition. *Trends Cogn Sci* 13:403–409. doi:10.1016/j.tics.2009.06.003

Todorovic A, Schoffelen J-M, van Ede F, Maris E, de Lange FP. 2015. Temporal expectation and attention jointly modulate auditory oscillatory activity in the beta band. *Plos One* 10:e0120288. doi:10.1371/journal.pone.0120288

Walter G, Cooper R, Aldrige VJ, McCallum WC, Winter AL. 1964. Contingent negative variation: An electric sign of sensorimotor association and expectancy in the human brain. *Nature*.

Warren S, Yacoub E, Ghose G. 2014. Featural and temporal attention selectively enhance task-appropriate representations in human V1. *Nat Commun* 5:5643–5643. doi:10.1038/ncomms6643

Wyart V, Nobre AC, Summerfield C. 2012. Dissociable prior influences of signal probability and relevance on visual contrast sensitivity. *Proc National Acad Sci* 109:3593–3598. doi:10.1073/pnas.1120118109